

## Authors responses (ACs) to RC1 Comments on amt-2021-339

We thank the reviewer for their careful reading of our manuscript and their comments. Each reviewer comment is reproduced in *italics* below, followed by our response in blue text.

### RC1: 'Comment on amt-2021-339', Anonymous Referee #1, 07 Dec 2021

The manuscript provides results derived from the NAOMI data analysis finalized to the measurement of the vertical profile of O<sub>3</sub> at Ny-Alesund in the microwave region.

Results are provided in terms of seasonal averages and compared to co-located SABER data in the thermal infrared (9.6  $\mu\text{m}$ ). The degree of consistency between the two datasets is summarized at the seasonal level.

SABER derived O<sub>3</sub> concentrations at 9.6  $\mu\text{m}$  are also compared to the ones derived at 1.27  $\mu\text{m}$ , showing differences comparable to SABER vs. NAOMI data.

Overall, the paper presents an interesting dataset, showing information that is incremental with respect of previous studies, towards a better understanding of the vertical distribution of O<sub>3</sub> in the Northern polar region. The comparison with the SABER dataset is important to establish eventual biases and effects affecting O<sub>3</sub> measurements in the mesosphere at twilight.

At the same time, the manuscript is unclear in some passages, and some ideas related to how NAOMI data products compare to the respective SABER ones could be better explicated.

#### Major comments:

*The manuscript does not sufficiently describe some key retrieval details. While the retrieval setting is fully described in Newnham et al. (2019) the manuscript would be clearer if some of the elements were reported in it: what covariance matrix is used for the O<sub>3</sub> profile? Are other parameters fitted? What linelist is used for RT calculations?*

The description of the retrieval methodology was kept brief as details are given in Newnham et al. (2019). However, we agree with the reviewer that adding further details to this manuscript would be helpful. The description in section 2.1.3 will be revised to include the following.

'Mesospheric O<sub>3</sub> profiles were retrieved from the NAOMI observations using version 2.2.58 of the Atmospheric Radiative Transfer Simulator (ARTS) (available at <http://www.radiativetransfer.org/>, last access: 8 August 2016) (Buehler et al., 2005, 2018; Eriksson et al., 2011) and the Qpack2 (a part of atmlab v2.2.0) software package (Eriksson et al., 2005) using the optimal estimation method (OEM) (Rodgers, 2000). The configuration of ARTS / Qpack2 for optimal estimation retrieval in the Ku-band region was described in Newnham et al. (2019) and specific details of the O<sub>3</sub> retrieval from NAOMI observations are given here. Adjusted parameters were O<sub>3</sub> VMR, frequency shift, and baseline slope. The Planck formalism was used for calculating brightness temperatures and atmospheric transmittance. Spectroscopic line parameters for ozone (O<sub>3</sub>), hydroxyl radical (OH), water

vapour (H<sub>2</sub>O), molecular nitrogen (N<sub>2</sub>), molecular oxygen (O<sub>2</sub>), and carbon dioxide (CO<sub>2</sub>) were taken from the high-resolution transmission (HITRAN) molecular absorption database (Gordon et al., 2017). For all molecules except OH the Kuntz approximation (Kuntz, 1997) to the Voigt line shape with a Van Vleck–Huber prefactor (Van Vleck and Huber, 1977) and a line cut-off of 750 GHz was used, which is valid for the pressures considered. The water vapour continuum parameterisation used the Mlawer–Tobin Clough–Kneizys–Davies (MT-CKD) model (version 2.5.2), which includes both foreign and self-broadening components (Mlawer et al., 2012). Collision-induced absorption (CIA) is the main contribution to the dry continua in the microwave range, and therefore the CIA parameterisations from the MT-CKD model (Clough et al., 2005) (version 2.5.2 for N<sub>2</sub> and CO<sub>2</sub> and version 1.0 for O<sub>2</sub>) were applied. Diagonal elements in the covariance of the O<sub>3</sub> VMR profiles were fixed to 1.5 ppmv. The off-diagonal elements of the covariance linearly decrease with a correlation length of a fifth of a pressure decade (approximately 3 km).’

The following citations will be added to the References section: -

Clough, S., Shephard, M., Mlawer, E., Delamere, J., Iacono, M., Cady-Pereira, K., Boukabara, S., and Brown, P.: Atmospheric radiative transfer modeling: a summary of the AER codes, *J. Quant. Spectrosc. Ra.*, 91, 233–244, 2005.

Gordon, I. E., Rothman, L. S., Hill, C., Kochanov, R. V., Tan, Y., Bernath, P. F., Birk, M., Boudon, V., Campargue, A., Chance, K. V., Drouin, B. J., Flaud, J.-M., Gamache, R. R., Hodges, J. T., Jacquemart, D., Perevalov, V. I., Perrin, A., Shine, K. P., Smith, M.-A. H., Tennyson, J., Toon, G. C., Tran, H., Tyuterev, V. G., Barbe, A., Császár, A. G., Devi, V. M., Furtenbacher, T., Harrison, J. J., Hartmann, J.-M., Jolly, A., Johnson, T. J., Karman, T., Kleiner, I., Kyuberis, A. A., Loos, J., Lyulin, O. M., Massie, S. T., Mikhailenko, S. N., Moazzen-Ahmadi, N., Müller, H. S. P., Naumenko, O. V., Nikitin, A. V., Polyansky, O. L., Rey, M., Rotger, M., Sharpe, S. W., Sung, K., Starikova, E., Tashkun, S. A., Vander Auwera, J., Wagner, G., Wilzewski, J., Wcislo, P., Yu, S., and Zak, E. J.: The HITRAN2016 molecular spectroscopic database, *J. Quant. Spectrosc. Ra.*, 203, 3–69, <https://doi.org/10.1016/j.jqsrt.2017.06.038>, 2017.

Kuntz, M.: A new implementation of the Humlicek algorithm for the calculation of the Voigt profile function, *J. Quant. Spectrosc. Ra.*, 57, 819–824, 1997.

Mlawer, E. J., Payne, V. H., Moncet, J.-L., Delamere, J. S., Alvarado, M. J., and Tobin, D. C.: Development and recent evaluation of the MT-CKD model of continuum absorption, *Philos. T. R. Soc. A*, 370, 2520–2556, 2012.

Van Vleck, J. and Huber, D.: Absorption, emission, and linebreadths: A semi-historical perspective, *Rev. Mod. Phys.*, 49, 939, <https://doi.org/10.1103/RevModPhys.49.939>, 1977.

*The manuscript does not sufficiently explore possible causes for the discrepancy with SABER 9.6 μm products. In Smith et al. (2013) that this work references, possible causes for this discrepancy are discussed, and it would be very valuable to do the same in this work to give a perspective on such discrepancies at twilight.*

The following paragraphs will be added to the Conclusions section, after line 379.

‘Possible reasons for the differences between mesospheric O<sub>3</sub> measured by the SABER 9.6 μm channel and other satellite datasets have been discussed by Smith et al. (2013). Here, we consider these reasons and other potential causes for observational differences in the context of our NAOMI ground-based measurements and comparisons between the

SABER 9.6  $\mu\text{m}$  and 1.27  $\mu\text{m}$  data products. The differences between observations can be categorised as those that occur due to systematic and random differences in coincident retrieved profiles and those caused by the different sampling by each instrument.

Our work uses the latest publicly available SABER v2.0 data products whereas Smith et al. (2013) used the earlier v1.07 dataset. The v2.0 processing includes improved Level 1 radiance profile calibration and improvements to the Level 2 procedures used to retrieve mesospheric temperatures in non-local thermodynamic equilibrium conditions as well as updated atomic oxygen, atomic hydrogen, and chemical heating algorithms. More information on the SABER data processing and retrieval schemes can be found on the instrument website: <http://saber.gats-inc.com>. The changes in the SABER v2.0 datasets should have improved the  $\text{O}_3$ , water vapour, and temperature profiles used in our analysis. However, we observe similar differences in  $\text{O}_3$  above  $\sim 60$  km as the earlier study (Smith et al., 2013) using v1.07 data, suggesting that significant uncertainties remain in SABER mesospheric  $\text{O}_3$ .

The SABER  $\text{O}_3$  processing schemes are complex and, despite recent improvements, the retrievals are highly dependent on knowledge of numerous photochemical and quenching rates. For the 9.6  $\mu\text{m}$   $\text{O}_3$  emission scheme, the SABER model includes spontaneous emission by over 340 radiative transitions, chemical pumping, collisional excitation, and quenching processes. The 1.27  $\mu\text{m}$  measurement is known to be prone to errors when  $\text{O}_3$  concentration is changing rapidly, including during sunrise and sunset (Zhu et al., 2007).  $\text{O}_3$  abundances in the upper mesosphere are also sensitive to temperature and atomic oxygen transport, which can vary rapidly and locally due to sunlight and tidal effects and may amplify sampling differences between different observations. Smith et al. (2013) show that sampling differences between instruments can lead to substantially different vertical profile structures and seasonal variations even when coincident comparisons indicate good agreement. In our work, we have matched up co-located NAOMI and SABER observations in terms of overlapping geographic location, SZA, and local observation time. However, sampling differences between the ground-based and satellite instruments inevitably remain and contribute to the observed  $\text{O}_3$  differences. Continuous atmospheric measurements from ground-based instruments such as NAOMI offer a complementary approach to satellite data analysis. Further work is needed to investigate and minimise instrument sampling differences, in particular local time and location effects that may be sensitive to the diurnal cycle in SZA. Studies focusing on  $\text{O}_3$  profiles during twilight and summer daytime conditions, when observations show large differences, are needed to address current uncertainties in mesospheric  $\text{O}_3$ .

The following citation will be added to the References.

Zhu, X., Yee, J.-H., and Talaat, E. R.: Effect of dynamical-photochemical coupling on oxygen airglow emission and implications for daytime ozone retrieved from 1.27  $\mu\text{m}$  emission, *J. Geophys. Res.*, 112, D20304, <https://doi.org/10.1029/2007JD008447>, 2007.

#### **Minor comments:**

*Line 165: how were SABER products binned?*

The SABER data were binned and averaged in the same way as the NAOMI datasets. For clarity, the sentence starting on line 165 will be rewritten as: -

'The SABER observations in the defined region were then binned and averaged into night-time, twilight, and daytime datasets within the defined winter, summer, and autumn periods, as was done for the NAOMI data (section 2.1.2).'

*Line 186-187: the retrieval shown in Fig. 3 is an average over a season, and this should be stated at this point for clarity.*

The text in lines 186–187 will be revised to 'The retrieval results for the seasonally-averaged 2017–18 winter night-time NAOMI spectrum is shown in **Figure 3**.'

*Line 188: noise level is not shown in Fig. 3b and should be reported. Furthermore, because this is a spectral average, is the noise scaled by, e.g., the square root of the number of measurements?*

Lines 187–188 will be revised as follows to report the noise level for the spectrum and residual differences, and to define the abbreviation 'RMS'.

'... with the root mean square (RMS) noise of the residual differences having the same value (2.4 mK) as the RMS baseline noise level of the seasonally-averaged NAOMI spectrum.'

*Line 189: the line in Fig. 3c seems green, not black.*

Thanks to the reviewer for pointing this out. The a priori line is indeed coloured green rather than black. Figure 3c has been revised to include the measurement uncertainty and total uncertainty as suggested in the reviewer's next comment (see response below). Lines 188–189 will be revised to '**Figure 3c** shows the retrieved (red line) and a priori (dashed green line) O<sub>3</sub> VMR profiles, the a priori uncertainty (green shading), the measurement uncertainty (medium blue shading), and the total uncertainty (light blue shading).'

The caption for the revised Figure 3 has also been updated to reflect the changes made to the figure.

*Figure 3: the uncertainty on the retrieved profile could be better shown in Fig. 3c instead of a separate panel (f and g), to be compared to the a-priori one. Also, a scale for MR should be shown (unless it is common to the AVK, in which case the axis caption should say "AVK and MR")*

The measurement uncertainty ( $\sigma_{obs}$ ) and total uncertainty ( $\sigma_{tot}$ ) of the retrieved ozone VMR profile have been added to Figure 3c as medium blue and light blue shading respectively. We propose keeping the individual plots of  $\sigma_{obs}$  and  $\sigma_{tot}$  (now presented in Figures 3g and 3h) to allow the actual uncertainty values to be seen more clearly than in the revised Figure 3c. A new panel (Figure 3e) has been added to show the measurement response (MR) more clearly, separate from the averaging kernels plot (Figure 3d).

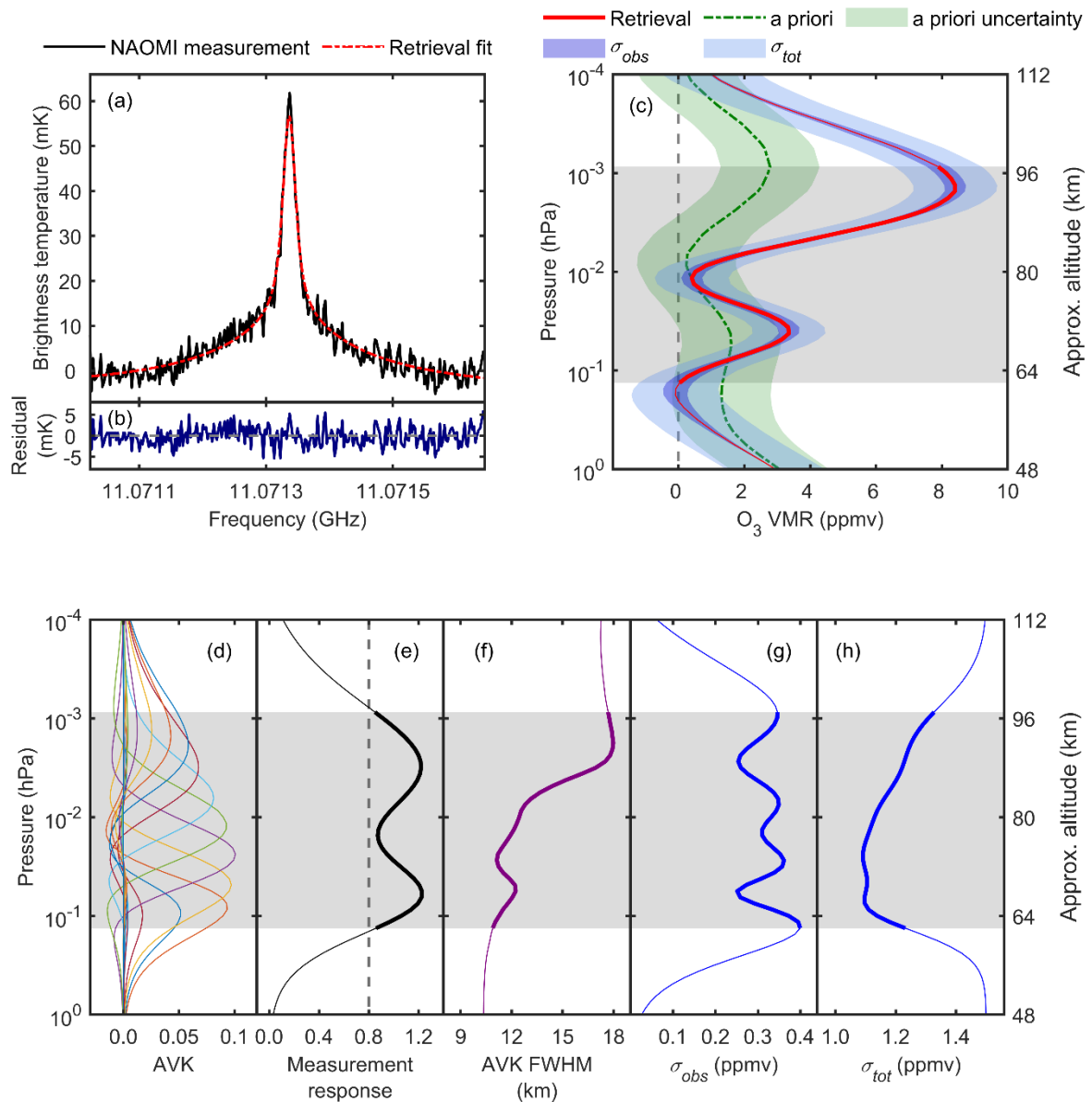


**Figure 3:** Ozone (O<sub>3</sub>) retrieval for NAOMI observations during 2017–18 winter night-time (29 December 2017 – 16 February 2018, SZA at altitude 90 km > 110°) conditions. The seasonal mean O<sub>3</sub> spectrum and retrieval fit is shown in (a), and the residual differences are shown in (b). The a priori and retrieved O<sub>3</sub> volume mixing ratio (VMR) profiles are shown in (c), where the green shading represents the a priori uncertainty ( $\pm 1.5$  ppmv). The medium blue and light blue shading show the profiles of O<sub>3</sub> VMR  $\pm$  measurement uncertainty ( $\sigma_{obs}$ ) and O<sub>3</sub> VMR  $\pm$  total uncertainty ( $\sigma_{tot}$ ) respectively. In (d) every sixth averaging kernel is shown and in (e) the measurement response (MR), with the vertical grey dashed line showing the cut-off for MR  $\geq 0.8$ . Panel (f) shows the full-width half maxima of each averaging kernel (AVK FWHM). The measurement uncertainty ( $\sigma_{obs}$ ) and total uncertainty ( $\sigma_{tot}$ ) are shown in (g) and (h) respectively. The grey shaded regions and thicker sections of the plotted curves in (c)–(h) indicate the pressure and altitude ranges where MR  $\geq 0.8$ .

Tables 1 to 3: the caption on top reports (ppmv) as a unit in brackets, however the one in bracket is the uncertainty. I would suggest to use a more traditional notation as the plus or minus sign for uncertainties to not to create confusion. On the same aspect, the uncertainties in the other figures seem very different from the ones reported in this table: it is not clear how are these uncertainties calculated, and it should be specified.

Thanks to the reviewer for pointing this out. The uncertainties in brackets in Tables 1–3 have been changed to  $\pm$ uncertainty, and the table captions revised accordingly. The following sentence will be added (~Line 257) to explain how the uncertainties are derived.

'For NAOMI the uncertainties are total error ( $\sigma_{tot}$ ) from the O<sub>3</sub> retrievals at the peak altitude and for SABER the estimated uncertainties are 20% of the peak VMR.'

Year(s)	Secondary O <sub>3</sub> peak				Tertiary O <sub>3</sub> peak			
	NAOMI		SABER		NAOMI		SABER	
	O <sub>3</sub> VMR (ppmv)	Altitude (km)	O <sub>3</sub> VMR (ppmv)	Altitude (km)	O <sub>3</sub> VMR (ppmv)	Altitude (km)	O <sub>3</sub> VMR (ppmv)	Altitude (km)
2017–18	8.4±1.3	94	12.0±2.4	95	3.4±1.1	70	2.6±0.5	71
2018–19	8.3±1.3	94	7.2±1.4	95	3.5±1.1	69	2.3±0.5	70
2019–20	10.7±1.3	93	11.9±2.4	94	3.8±1.1	69	2.7±0.5	72

**Table 1:** Secondary and tertiary ozone peak VMR and altitudes from NAOMI and SABER 9.6  $\mu$ m observations during winter night-time (within 15 December–15 March, SZA at altitude 90 km > 110°) conditions for 2017–18, 2018–19, and 2019–20. The  $\pm$  figures after VMR values are uncertainties.

Year(s)	Secondary O <sub>3</sub> peak				Tertiary O <sub>3</sub> peak			
	NAOMI		SABER		NAOMI		SABER	
	O <sub>3</sub> VMR (ppmv)	Altitude (km)	O <sub>3</sub> VMR (ppmv)	Altitude (km)	O <sub>3</sub> VMR (ppmv)	Altitude (km)	O <sub>3</sub> VMR (ppmv)	Altitude (km)
2017–18	7.9±1.3	94	8.8±1.8	94	4.0±1.1	70	2.7±0.5	73
2018–19	6.9±1.3	94	7.8±1.6	95	3.0±1.1	71	2.1±0.4	69
2019–20	9.5±1.3	94	10.7±2.1	95	3.8±1.1	70	2.9±0.5	73

**Table 2:** Secondary and tertiary ozone peak VMR and altitudes from NAOMI and SABER 9.6  $\mu$ m observations during winter twilight (within 15 December–15 March, 75° ≤ SZA at altitude 90 km ≤ 110°) conditions for 2017–18, 2018–19, and 2019–20. The  $\pm$  figures after VMR values are uncertainties.

Year(s)	Secondary O <sub>3</sub> peak				Tertiary O <sub>3</sub> peak			
	NAOMI		SABER		NAOMI		SABER	
	O <sub>3</sub> VMR (ppmv)	Altitude (km)	O <sub>3</sub> VMR (ppmv)	Altitude (km)	O <sub>3</sub> VMR (ppmv)	Altitude (km)	O <sub>3</sub> VMR (ppmv)	Altitude (km)
2017	4.4±1.2	93	9.4±1.9	95	1.5±1.0	72	1.3±0.3	71
2018	5.3±1.2	93	9.0±1.8	94	2.1±1.0	70	1.4±0.3	72
2019	1.3±1.3	95	8.0±1.6	94	1.7±1.1	65	1.4±0.3	72

**Table 3:** Secondary and tertiary ozone peak VMR and altitudes from NAOMI and SABER 9.6 μm observations during autumn twilight (within 15 September–15 November, 75° ≤ SZA at altitude 90 km ≤ 110°) conditions in 2017–19. The ± figures after VMR values are uncertainties.

*Table 4: is it possible to report SABER uncertainties in the same fashion of the previous tables, and the values for the other peak?*

Uncertainties in the SABER secondary ozone peak VMR values have been added to Table 4, using the ± uncertainty notation. Regarding the other peak, the tertiary ozone layer is seasonal and forms during winter months at mid- to high- latitudes. The comparison between SABER 9.6 μm and 1.27 μm observations has been carried out for summer and autumn periods, when the tertiary layer is not present. Therefore, values for the tertiary peak are not presented.

	Year(s)	SABER 9.6 μm		SABER 1.27 μm	
		O <sub>3</sub> VMR (ppmv)	Altitude (km)	O <sub>3</sub> VMR (ppmv)	Altitude (km)
Summer, day	2017	0.95±0.19	97	0.85±0.17	98
	2018	1.07±0.21	97	0.99±0.20	99
	2019	1.18±0.24	96	1.10±0.22	98
Summer, twilight	2017	0.71±0.14	97	0.67±0.13	98
	2018	0.73±0.15	97	0.64±0.13	98
	2019	0.88±0.18	96	0.79±0.16	97
Autumn, twilight	2017	1.05±0.21	96	0.87±0.17	97
	2018	1.08±0.22	96	0.90±0.18	97
	2019	1.11±0.22	96	1.00±0.20	98

**Table 4:** Secondary ozone peak VMR and altitudes from SABER 9.6 μm and 1.27 μm observations during summer daytime (within 15 April–15 July, SZA at altitude 90 km < 75°), summer twilight (within 15 April–15 July, 75° ≤ SZA at altitude 90 km ≤ 110°), and autumn twilight (within 15 September–15 November, 75° ≤ SZA at altitude 90 km ≤ 110°) conditions for 2017–19. ± figures after the VMR values are uncertainties.

Citation: <https://doi.org/10.5194/amt-2021-339-RC1>